Association for Information and Image Management

1100 Wayne Avenue, Suite 1100
Silver Spring, Maryland 20910

301/587-8202

Centimeter

1 2 3 4 5 6 7 8 9 10 11 12 13 14 15 mm

1 2 3 4 5

Inches

MANUFACTURED TO AIIM STANDARDS
BY APPLIED IMAGE, INC.

1 of 1

PERFORMANCE OF THE NIF PROTOTYPE BEAMLET*

Bruno M. Van Wonterghem, John R. Murray,
D. Ralph Speck, and John H. Campbell
University of California
Lawrence Livermore National Laboratory
P.O. Box 5508, L-490
Livermore, CA 94551-9900
(510) 423-9494 / FAX (510) 423-6506

ABSTRACT

Beamlet is a full scale single beam prototype laser system, built to demonstrate the laser technology and performance of the 192 beam National Ignition Facility (NIF) fusion laser driver. Both laser systems apply multipass amplifier architectures. By passing the beam four times through the large aperture amplifier sections, the small signal gain during the first few passes is used efficiently to reduce expensive staged amplifier chains. The beamlet prototype laser integrates results of development programs for large aperture components: large aperture optical switch, polarizers, 2 x 2 multisegment amplifiers and new pulse generation and pre-amplification techniques. We report on performance test results of the recently completed 1ω-laser section of Beamlet.

INTRODUCTION

The Department of Energy is proposing to build a National Ignition Facility that will be used to conduct laser driven Inertial Confinement Fusion (ICF) experiments with the goal of achieving ignition and propagation of a thermonuclear fusion burn. The NIF driver will be a Nd-glass laser consisting of 192 individual "beamlets" built into four compact arrays containing 48 of these beamlets.[1] The Beamlet laser, which is discussed in this paper, is a full-scale, single-aperture scientific prototype of the NIF design (Fig. 1 and Fig. 2). The goal of the Beamlet is to demonstrate the laser technology and laser performance of the proposed NIF, specifically at the third harmonic wavelength (351 nm) where damage on the KDP tripler limits the fluence and performance of the system.

Current ICF driver Nd-glass lasers, for example the LLNL NOVA laser, use a master-oscillator, power-amplifier (MOPA) laser architecture.[2] In contrast the Beamlet (i.e. NIF) has a multipass design[3] utilizing angular multiplexing to separate spots in the focal plane of a spatial filter in the cavity. The pulse is injected at the mid-plane of the spatial filter (Fig. 1). After four passes through the amplifiers, the pulse is switched out of the cavity using a unique, full-aperture (35-cm) plasma electrode Pockels cell.[4] The pulse then makes a single pass through a "booster" amplifier section that is driven heavily into saturation and finally, after passing through another spatial filter, will be converted to 351 nm using a Type I/II KDP/KD*P frequency conversion scheme. Activation of the Beamlet frequency converter is scheduled for completion by September 1994. The Beamlet uses a spatially-square beam and will support experimental tests over a range of beam sizes up to 35 x 35 cm^2. All activation test described here have been performed using a 34 x 34 cm^2 size, as limited by vignetting in the hard aperture of the Pockels cell.

In a next phase, the Beamlet prototype will be expanded to include high fluence 1ω transport mirrors, and a full 3ω focal spot evaluation chamber that includes the NIF final 3ω focussing and phase plate optics. In a separate experimental campaign, alternative small aperture switch geometries will be evaluated.

BEAMLET CAVITY

The Beamlet multi-pass cavity was completed in March 1993, following extensive on-line tests of the PEPC optical switch. The amplifier activation test included the complete cavity with 11 amplifier slabs, the optical switch, transport optics and transport filter. A single inactive booster slab was needed to maintain alignment of the optical axis. Diagnostics are available at each end of the cavity recording energy, pulse shape and near field image of each pass in addition to a complete diagnostics package at the output of the transport spatial filter.

The 79 cm long Beamlet slabs have high gain-length products, and suffer from ASE induced gain depletion near the edges of the slabs.[5] At a flashlamp pump explosion fraction of 20%, this effect leads to a significant small-signal

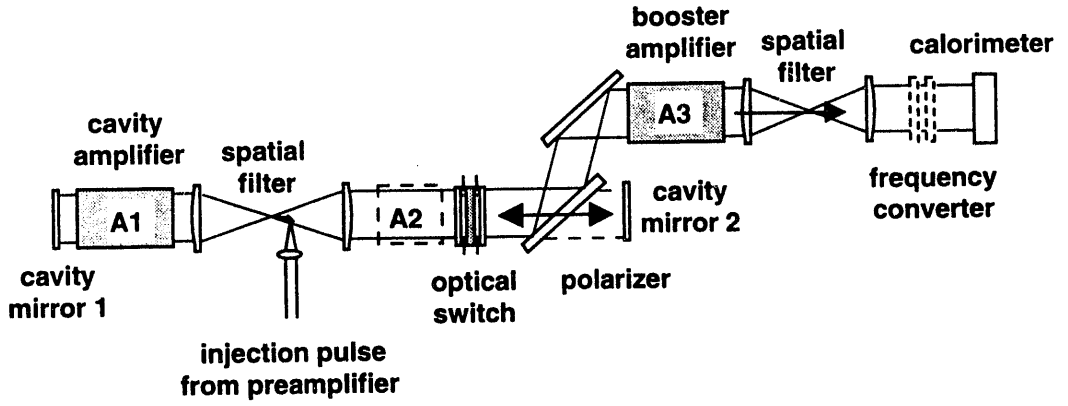

Figure 1. Layout of the Beamlet prototype amplifier chain. The present configuration has eleven amplifiers in position A1 and five in A3. The actual laser is folded using two mirrors between the polarizer and the booster amplifier section. The total cavity length between mirrors is 36 meters.

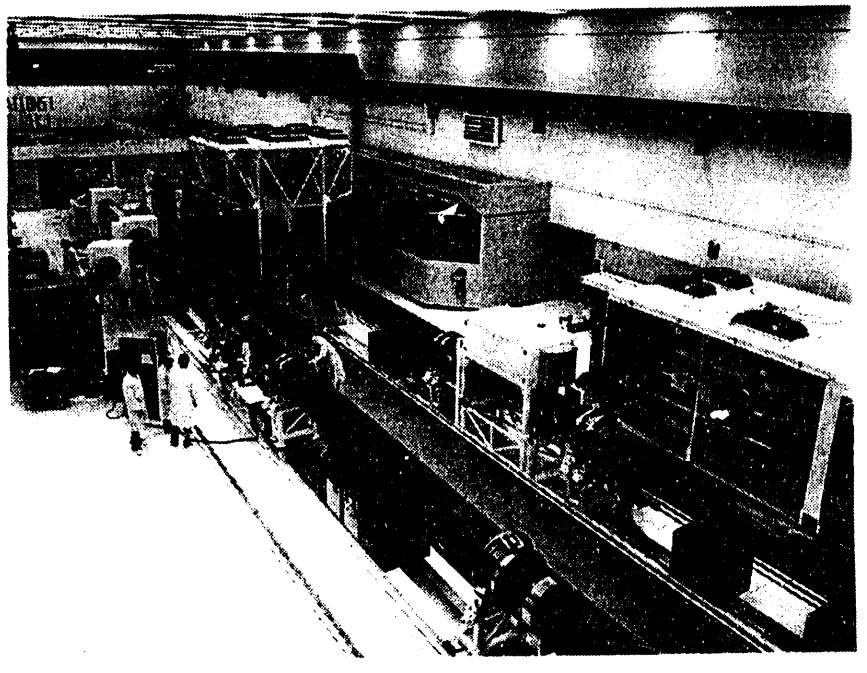

Figure 2. Photo of the Beamlet laser.

gain roll-off for the total of 44 slabs in a cavity amplification path. Since the laser is essentially optimized to operate at optical damage limits, the total energy output is maximized when the fluence at the output of the system is uniform over the beam aperture. A spatial beam shaping system was implemented in the preamplifier section to increase the fluence near the edges of the beam. A simple scheme using parabolic shaped metallic transmission filters with an edge-to-center transmission ratio of 2:1 was shown to produce nearly flat output fluence distributions.

The lower curve in Fig. 3 shows the performance of the multipass amplifier using 3-ns pulses. Pulse shapes were temporally compensated for gain saturation in the amplifiers, using integrated optical modulators in the pulse forming section of the pre-amplifier.[6] The multi-segment amplifiers[5] were operated at 20% lamp pumping explosion fraction, leading to an aperture averaged single-pass, small-signal gain of 15 in the cavity. Gain saturation is small in the cavity, since the maximum output fluence is approximately equal to the effective saturation fluence of the Brewster angle LG-750 slabs (6.8 J/cm^2). The near field peak-to-average fluence modulation was 1.25 at average output fluences up to 6.2 J/cm^2.

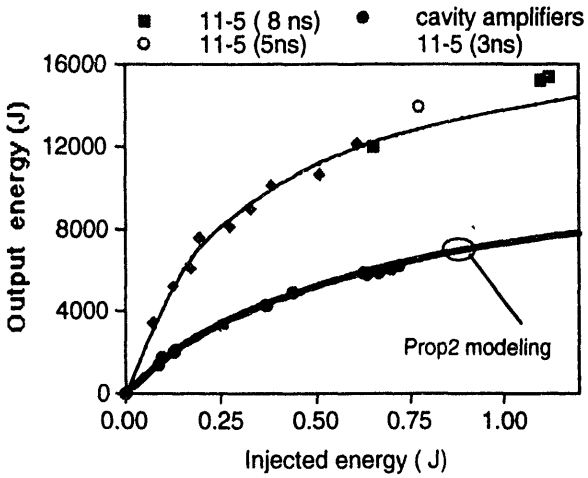

Figure 3. Performance curves of the multipass amplifier (lower curve), and the complete 11-5 amplifier system at 1ω. 2:1 spatial beam shaping was used for every shot result shown. Modeled results are shown for the cavity amplifier.

Parasitic oscillations are a concern in multi-pass amplifiers. Angular multiplexing uses a small pointing offset to separate the focal spots of the different passes. The number of passes is limited to 5 by a beam dump located near the focal plane of the spatial filter. The injection path is isolated using two faraday isolators. All surfaces near the focal plane have a laser light absorbing surface and are sufficiently tilted to avoid back reflections. The Beamlet prototype has been tested up to a cavity amplifier round-trip gains of 400 without problems. Shot pinholes had a 3.6 mm diameter in a high density carbon substrate.

Ghost reflections from spatial filter lens surfaces illuminate the pinhole plane and lead to small beams that propagate through various passes in the cavity. The existence of these ghost beams has been confirmed by a dedicated return signal diagnostic located near the injection system. Breakdown in the nitrogen atmosphere of the beam tubes can be induced by ghost foci of pass 2 and 3 back-reflections. In a multi-pass system, the pulse encounters these plasma spots after a 240 ns round-trip. During this time the plasma has time to expand to several mm radius. Near field images of the cavity amplifier output beam confirm the existence of these plasmas as small obscurations in the beam.

1ω PERFORMANCE WITH BOOSTER AMPLIFIER

The performance curve of the system with 5 additional booster amplifiers is shown on Fig. 3. All shots used spatial gain pre-compensation, and temporal shaping to obtain square output pulses. At the highest energy, 15.4 kJ, a 12.5:1 pulse shape contrast was required to compensate pulse shape distortion by saturation in the amplifiers. The boosters amps are run in saturated mode and approximately 1-1.5 kJ is extracted per slab. Modeling of the performance improvement due to higher pulsed power transfer efficiency to the booster amplifier is in progress.

Beam quality is usually characterized by two parameters: the near field beam fluence distribution as obtained from beam images, and the wavefront aberration or beam divergence which determines the focal spot size of the beam. Both will be discussed in the following sections.

NEAR FIELD BEAM MODULATION

Figure 4 shows a near field 1ω-output beam image, obtained on a 12 kJ (3 ns) shot. The well defined apodized beam edges are created in the pre-amplifier pulse-shaping section using precise photo-lithographically created serrated aperture in combination with appropriate spatial filtering. The experimental fill factor of the beam exceeds 84%. The beam displays two sets of characteristic features: vertical curved lines, which are caused by machining marks in the Pockels cell KDP crystal, and weak horizontal lines, caused by small tool finishing of amplifier slabs. The spatial frequency of the KDP machining marks is 6 mm, just below the cut-off frequency of the 200 μrad pinholes used in the cavity and transport spatial filters. Horizontal and vertical line-outs

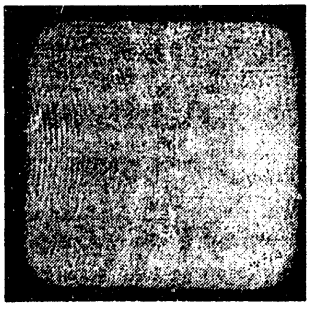

Figure 4. Near-field image of the 34 x 34 cm^2 output beam on a 12 kJ (3-ns) shot. The curved features are caused by machining marks on the optical switch KDP crystal.

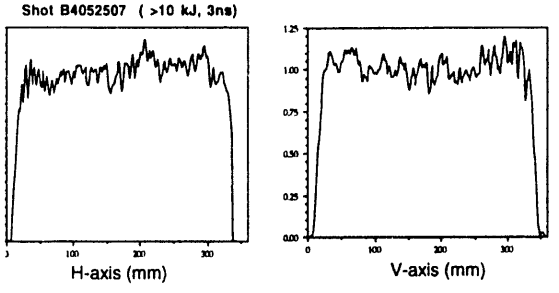

Figure 5. Near-field beam profile line-outs show the low fluence modulation typical for the Beamlet prototype.

through a beam image of a 10 kJ (3 ns) shot (Fig. 5), clearly indicate the periodic modulation induced by these noise sources. The laser slabs are presently being re-worked to remove the small tool marks, and development is also ongoing to eliminate the KDP machining marks.

The peak-to-average modulation of 1.25 at low fluence and intensity, increases to 1.35 at 12 J/cm^2 in a 3 ns pulse (4 GW/cm^2). This is the maximum operating fluence at 3 ns, based on cavity polarizer damage threshold and nonlinear ripple growth as determined by B-integral effects. The nonlinear-induced phase shift, or B-integral, between two consecutive spatial filter pinholes (ΔB) reaches a maximum of 1.85 on the output pass through the booster amplifier section. The cumulative B-integral through the laser system (ΣB) approaches 4. The last number applies to growth of spatial noise transmitted by the pinholes: i.e. the above mentioned KDP machining marks. A separate set of experiments used short pulses to demonstrate ripple growth at intensities exceeding 5 GW/cm^2. During these experiments, the beam was allowed to accumulate a B-integral value exceeding 3.5 by propagation through the inactive booster amplifiers slabs. Various beam images were statistically analyzed to create cumulative power distribution plots as shown in Fig. 6. The total energy fraction is plotted as function of normalized local fluence in the beam. The data sets display the small signal low-fluence modulation (1.6 J/cm^2, 3 ns), the high-fluence, low-intensity case (15.4 J/cm^2, 8 ns), and the high-fluence, high-intensity case (12 J/cm^2, 3 ns). As expected, amplifier saturation tends to reduce the modulation slightly at high fluence, if the intensity, and therefore B-integral, remains small. Nonlinear modulation however is exponentially dependent on the B-integral, and clearly dominates the distribution at higher intensities. For comparison, the fourth curve shows the modulation distribution observed in a ripple growth experiment (1.1 J/cm^2, 0.2 ns). Even at 12 J/cm^2 (3 ns), the fluence modulation is sufficiently small to meet damage threshold safety margins, despite the presence of extra noise sources. We expect the modulation to be reduced significantly by either removing the noise sources in the optics, or by using tighter spatial filtering[7] using (150 μr pinholes).

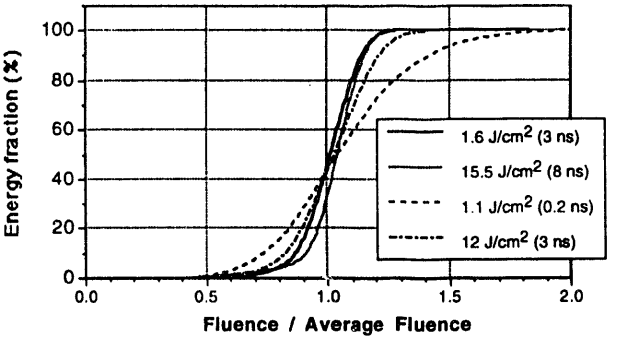

Figure 6. Cummulative power distributions for shots at various operation regimes. Solid line represents the low power distribution. The dotted line demarkates a slight smoothing effect at high saturation conditions and low B integral. The evolution of the modulation at high B-integral is clearly seen for the 12 J/cm^2 (3ns), and 1.1 J/cm^2 (0.2 ns) case. The last case was performed with inactive booster amplifiers.

BEAM DIVERGENCE

The second parameter that characterizes beam quality, is the wavefront aberration in the optical system at the time of the shot. This involves static aberrations introduced by optical components, slow thermal effects caused by heat dissipation in the amplifiers, turbulence in the beam line, and fast pump-induced aberrations in the amplifier slabs. The Beamlet prototype has a 39 actuator deformable mirror in the injection beam path[8] to test wavefront correction techniques in large-aperture pulsed laser systems. Using a matched Hartmann

wavefront sensor in the 1ω-output diagnostics, static and slowly varying aberrations can be corrected before a laser shot in closed loop using the CW alignment laser or the pulsed front-end beam. The wavefront aberration was determined using a calibrated Hartmann sensor, in addition to an independent radial shearing interferometer, and indirectly by measuring the far-field intensity distribution.

Most of the activation shots were fired with precorrection for static aberrations less than 15 minutes before shot-time. Figure 7 shows a typical far-field image of a shot, as disturbed by dynamic pump induced wavefront distortion. 95 % of the beam's energy was contained in a ±35 μrad angle, which meets ±50 μrad divergence requirements for efficient type I/II frequency tripling. Analysis of the radial shearing interferograms shows a P-V wavefront aberration of 1.6 ± 0.2 waves with a 0.4 ± 0.1 waves RMS value. The actual wavefronts display the expected W-shape along the long axis of the amplifier slabs (H), as shown in Fig. 8.

Slight variations have been observed on successive shots during the course of a day. Shots were fired at irregular intervals, between 2 and 4 hours, with incomplete relaxation of thermal gradients in the amplifier slabs. Even under these uncontrolled circumstances, precorrection using wavefront

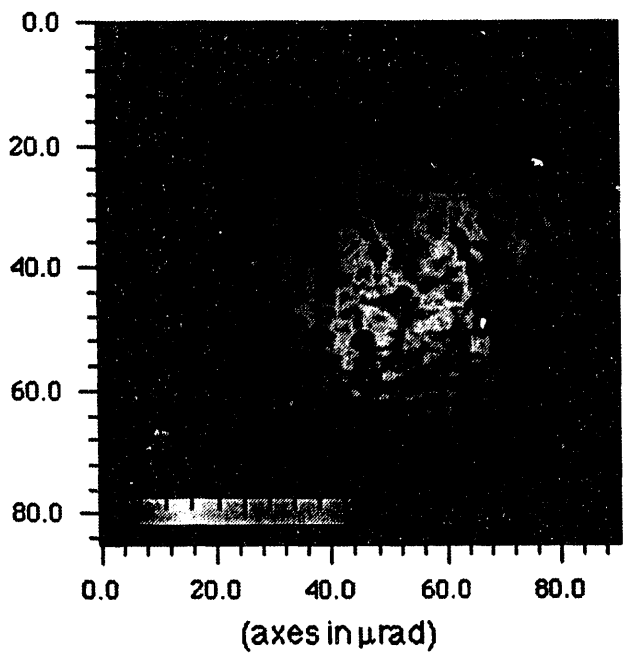

Figure 7. Focal plane image of a typical shot. No precorrection has been applied for dynamic beam steering effects in the amplifiers. Approximately 95% of the energy is contained in a ± 35 μrad divergency angle.

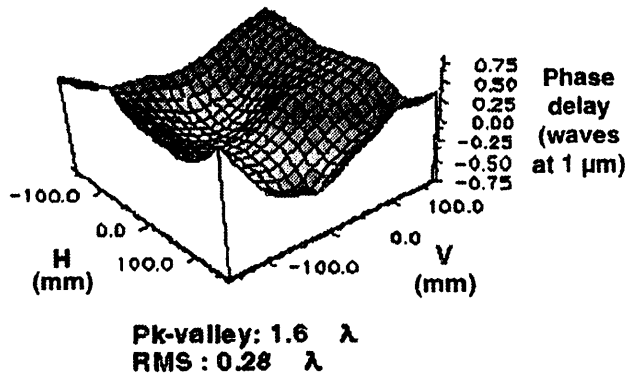

Figure 8. Reconstructed 1ω output beam wavefront of a 9 kJ shot showing phase delay in waves as a function of beam aperture coordinates. Peak-to-valley aberration is 1.6 waves, with 0.28 waves RMS. The W-shaped aberration along the H-axis is the typical pump-induced aberration observed from disk amplifier slabs. Data were obtained using a 77-element Hartmann sensor. (The surface curve is an interpolation between the discrete data points.)

data obtained on a previous shot, improves the beam divergence significantly. Preliminary data show a reduction of the beam divergence angle by 40% to ± 20 μrad. Strehl ratios up to 0.1 have been observed with 20% of the energy located within the radius of the central Airy disk. Further evaluation of the results will establish optimum circumstances for dynamic wavefront precorrection. Wavefront aberration caused by nonlinear phase modulation accumulated during the amplification of a pulse with non uniform intensity profile cannot be precorrected using this technique, and will finally limit its performance.

CONCLUSION

The 1ω section of the NIF Beamlet prototype has been assembled and completed. We successfully demonstrated its performance at the 3-ns design point of the prototype system. Using 11 slabs in a four-pass amplifier cavity with a full aperture optical switch and a 5-slab booster amplifier, the system produced fluences exceeding 12 J/cm^2 at 1ω. High beam quality is maintained as defined by the peak-to-average fluence modulation and wavefront aberration. We demonstrated several new pre-compensation techniques in the preamplifier that allow control over fill factor, wavefront and temporal shape of the output beam. Key performance parameters have been investigated at high fluence (15.5 J/cm^2), and high intensity (5.5 GW/cm^2) generating important results to validate the NIF design model. Table 1 summarizes several experimental results and parameters, as compared to their equivalent NIF design requirements.

Table 1. Comparison of Beamlet prototype 1ω performance parameters and NIF requirements. Beamlet prototype parameters are obtained for 3-ns-square output pulses, while NIF requirements are based on the equivalent pulse length of a more complex shaped pulse.

Amplifier configuration (cav A1-A2-booster A3)	Beamlet 11-0-5	NIF 9-5-5
High 1ω fluence	13.2 J/cm^2	13.3
(equivalent) pulse duration	(5.0 ns)	(5.1 ns)
Beam area (half power points)	1027 cm^2	1280 cm^2
Near field fluence modulation (pk-to-avg)	1.25-1.35	1.5
Spatial gain compensation contrast	3:1	5:1
Beam divergence:		
wavefront precorrection	±20 μrad	±35 μrad
static correction only	±35 μrad	
Phase modulation bandwidth	30 GHz	30 GHz
Cavity optical switch efficiency	99.6 %	99.5 %
To be demonstrated (summer 1994)		
High 3ω fluence	7.4 J/cm^2	8
(equivalent) pulse duration	(3.0 ns)	(3.6 ns)

ACKNOWLEDGMENTS

We thank the Beamlet operations, diagnostics, controls and pulsed power teams for their effort during the system activation, in addition to all the people who worked in the component development groups responsible for the amplifiers, large optics and Pockels cell. We acknowledge I.C. Smith, visiting researcher of the AWE UK for his contribution to the Beamlet diagnostics. We appreciate the discussions with J.T. Hunt, K. Manes, and the support from the U-AVLIS wavefront control group in activating the Adaptive Optics System.

*This work is performed under the auspices of the US. Department of Energy by the Lawrence Livermore National Laboratory under contract No. W-7405-ENG-48.

REFERENCES

1. National Ignition Facility Conceptual Design Report, Vol. 1-5, Lawrence Livermore Laboratory Report No. UCRL-PROP-117093, May 1994.

2. J.T. Hunt and D.R. Speck, "Present and Future Performance of the NOVA Laser System" Opt. Engineering, **28**, 462-468, (1989).

3. J.R. Murray, J.H. Campbell, D.N. Frank, J.T. Hunt and J.B. Trenholme, "The Nova Upgrade Beamlet Demonstration Project" ICF Quarterly Report Vol 1(3), Lawrence Livermore Laboratory Report UCRL-LR-105821-91-3.

4. M.A. Rhodes, J.J. DeYoreo, B.W. Woods and L.J. Atherton "Large-Aperture Optical Switch for High-Energy, Multipass Laser Amplifiers" ICF Quarterly Report, Vol 2(1), 1992, Lawrence Livermore Laboratory Report UCRL-LR-105821-92-1.

5. A.C. Erlandson, K.S. Jancaitis, R.W. McCracken and M.D. Rotter, "Gain Uniformity and Amplified Spontaneous Emission in Multi-segment Amplifiers", ICF Quarterly Report, Vol. 2 (3), pp. 105-114, (1992); LLNL Report UCRL-LR-105821-92-3.

6. R.B. Wilcox, D.F. Browning, D.R. Speck, W. Behrendt, B.M. Van Wonterghem: "Fusion laser oscillator and pulse-forming system using integrated optics," Laser Coherence Control: Technology and Applications, H.T. Powell and T.J. Kessler Eds., SPIE Proc. Vol. 1870, 1993. (UCRL-JC-111398).

7. J.T. Hunt, J.A. Glaze, W.W. Simmons, and P.A. Renard, "Suppression of self-focusing through low-pass spatial filtering and relay imaging," Appl. Opt. Vol. 17, p 2053, 1978.

8. J.T. Salmon, E.S. Bliss, T.W. Long, E. Orham, R.W. Presta, C.D. Swift and R.S. Ward, "Real-time wavefront correction system using a zonal deformable mirror and a Hartmann sensor," in Proceedings SPIE Conference on Active and Adaptive Optical Systems, San Diego, CA, Vol. 1542, p. 459 (1991).

DATE
FILMED
10/5/94

END